Journal of Biomolecular Screening

http://jbx.sagepub.com

Label-Free Assays on the BIND System

Brian T. Cunningham, Peter Li, Stephen Schulz, Bo Lin, Cheryl Baird, John Gerstenmaier, Christine Genick, Frank Wang, Eric Fine and Lance Laing

J Biomol Screen 2004; 9; 481
DOI: 10.1177/1087057104267604

The online version of this article can be found at:
http://jbx.sagepub.com/cgi/content/abstract/9/6/481

Published by:
SAGE
http://www.sagepublications.com

On behalf of:
SBS
Society for Biomolecular Sciences

Label-Free Assays on the BIND System

BRIAN T. CUNNINGHAM, PETER LI, STEPHEN SCHULZ, BO LIN, CHERYL BAIRD, JOHN GERSTENMAIER, CHRISTINE GENICK, FRANK WANG, ERIC FINE, and LANCE LAING

Screening of biochemical interactions becomes simpler, less expensive, and more accurate when labels, such as fluorescent dyes, radioactive markers, and colorimetric reactions, are not required to quantify detected material. SRU Biosystems has developed a biosensor technology that is manufactured on continuous sheets of plastic film and incorporated into standard microplates and microarray slides to enable label-free assays to be performed with high throughput, high sensitivity, and low cost per assay. The biosensor incorporates a narrowband guided-mode resonance reflectance filter, in which the reflected color is modulated by the attachment/detachment of biochemical material to the surface. The technology offers 4 orders of linear dynamic range and uniformity within a plate, with a coefficient of variation of 2.5%. Using conventional biochemical immobilization surface chemistries, a wide range of assay applications are enabled. Small molecule screening, cell proliferation/cytotoxicity, enzyme activity screening, protein-protein interaction, and cell membrane receptor expression are among the applications demonstrated. (*Journal of Biomolecular Screening* 2004:481-490)

Key words: Biomolecular Interaction Detection system, BIND, biosensors, pharmaceutical screening, label-free detection

INTRODUCTION

THE VAST MAJORITY OF ASSAYS currently used in pharmaceutical screening involve the usage of some sort of label to enable quantization of protein, DNA, small molecules, or cells. Typical labeling methods include the use of fluorophores, radioligands, and secondary reporters. In contrast with the large variety of labeled methods, there are relatively few methods that allow detection of molecular and cellular interactions without labels. Label-free detection removes experimental uncertainty induced by the effect of the label on molecular conformation, blocking of active binding epitopes, steric hindrance, inaccessibility of the labeling site, or the inability to find an appropriate label that functions equivalently for all molecules in an experiment.[1] Label-free detection methods greatly simplify the time and effort required for assay development while removing experimental artifacts from quenching, shelf life, and background fluorescence.[2]

Label-free detection generally involves the use of a transducer that is capable of directly measuring some physical property of a chemical compound, DNA molecule, peptide, protein, or cell. For example, all biochemical molecules and cells have finite mass, volume, viscoelasticity, dielectric permittivity, and conductivity that can be used to indicate their presence or absence using an appropriate sensor. The sensor functions as a transducer that can convert one of these physical properties (such as the mass of a substance deposited on the sensor's active surface) into a quantifiable signal that can be gathered by an appropriate instrument (such as a current or voltage that is proportional to the deposited mass).

Optical biosensors are designed to produce a measurable change in some characteristic of light that is coupled to the sensor surface. The advantage of this approach is that a direct physical connection between the excitation source (the source of illumination of the sensor), the detection transducer (a device that gathers reflected or transmitted light), and the transducer surface itself is not required. Without the need for electrical connections to the biosensor and associated complications of packaging, devising systems for interfacing the sensor with fluid exposure methods becomes greatly simplified. Rather than detecting mass directly, all optical biosensors rely on the dielectric permittivity of detected substances to produce a measurable signal.[3]

Adoption of a biosensor technology for most applications in diagnostics or pharmaceutical screening will be driven, to some extent, by the cost of performing an individual assay. For a "primary screen" used in the pharmaceutical research industry, for example, a screening campaign to determine a set of candidate chemicals that have a desired affinity level for a protein can involve more than 1 million assays. Researchers working on high-volume industrialized assays describe the need to minimize the cost per data point in such a campaign. Although optical biosensors offer tremendous advantage over labeled assay technologies by not requiring the use

SRU Biosystems, 14A Gill Street, Woburn, Massachusetts.

Received Feb 19, 2004, and in revised form Apr 8, 2004. Accepted for publication Apr 26, 2004.

Journal of Biomolecular Screening 9(6); 2004
DOI: 10.1177/1087057104267604

of tag reagents, the cost of the transducer used in each assay must be low enough to be used economically on a wide scale. This cost goal is an extreme challenge to the wide acceptance of optical biosensors, which are often high-precision optical components fabricated from expensive materials (such as glass, silicon, or optical fiber) using highly exacting processes such as photolithography, dielectric or metal deposition, and plasma etching. Even if a sensor is inexpensive to fabricate, the cost of packaging and testing must also be efficient. Therefore, for widest acceptance, an optical biosensor technology must be designed to be compatible with mass production methods using inexpensive materials such as plastics, so they can be used 1 time before disposal.

The throughput of a sensor system will also determine its usefulness in large pharmaceutical screening campaigns or for diagnostic tests in which a test sample must be measured for the contents of many different proteins. A biosensor embedded within a flow chamber will have a throughput that is limited by the number of parallel flow channels and the time required to flush reagents away from a previous assay, to regenerate the sensor surface, and to introduce a new test sample. Cuvette-based systems will have throughput limited by the number of cuvettes that can be operated in parallel. For example, cuvettes can provide much greater parallelism than a flow cell-based system if the cuvette is a well within a standard 96-, 384-, or 1536-well microplate.

Assay throughput can be further improved by nearly 2 orders of magnitude using spot-based multiplexing methods if the biosensor approach has the ability to measure high-resolution images of binding on its surface. If the distance that electromagnetic energy is allowed to travel laterally across the sensor surface is intentionally limited to a few microns, it is possible to take independent measurements of binding on the sensor surface from locations that are separated by distances no greater than only a few microns. Using tools that have the ability to deposit small spots of immobilized protein reagents (typical spot sizes are 100-500 μm in diameter) in an *x-y* grid across the sensor surface, each spot can be measured separately with an imaging biosensor readout instrument. With this method, a biosensor area of as little as 1 cm^2 can be used to perform several hundred assays in parallel, thereby dramatically improving the throughput of the system compared to single-channel flow cell-based systems. Image-based readout can be especially advantageous for obtaining high throughput when the imaged area can be increased to an entire 1 × 3-inch microscope slide or an entire microplate surface, where each microplate well can hold 10 to 100 spots.[4]

The ability to perform high-sensitivity detection of biochemical interactions in a format that concurrently provides high throughput and low cost/assay would enable label-free optical biosensor technology to address applications that have not been previously feasible on a commercial basis. In this article, we present a Biomolecular Interaction Detection (BIND) system based on an approach that uses a guided-mode resonant filter (GMRF) biosensor that is manufactured from continuous sheets of plastic film and incorporated into standard 96- and 384-well microplate formats for compatibility with standard robotic liquid-handling systems used in screening applications. The system uses single-use disposable biosensor labware and a simple, robust microplate reader instrument that is configured for compatibility with robotic microplate handlers. An advanced microplate reader with high-resolution imaging capability has also been developed for multiplexed assays and label-free microarrays. In this article, we describe the operation of the biosensor, sensor manufacturing, and the design of the readout instrument. Example assays for using the BIND systems for protein-protein interaction characterization, small molecule screening, and cell expression screening are also described.

MATERIALS AND METHODS

Guided-mode resonant filter biosensor

A new class of optical biosensors, based on the unique properties of optical device structures known as "photonic crystals," has been recently developed.[5,6] A photonic crystal is composed of a periodic arrangement of dielectric material in 2 or 3 dimensions.[7,8] If the periodicity and symmetry of the crystal and the dielectric constants of the materials used are chosen appropriately, the photonic crystal will selectively couple energy at particular wavelengths while excluding others.[9] The applications of structures such as these are numerous, including integration with lasers to inhibit or enhance spontaneous emission, waveguide angle-steering devices, and narrowband optical filters.[10-14] A photonic crystal structure geometry can be designed to concentrate light into extremely small volumes and to obtain very high local electromagnetic field intensities. These devices are often referred to as "sub-wavelength surfaces" (SWS) or as "nanostructure surfaces" because typical dimensions are smaller than the wavelength of light that they manipulate.

To adapt a photonic crystal device to perform as a biosensor, some portion of the structure must be in contact with a liquid test sample. By attaching biomolecules or cells to the portion of the photonic crystal where the locally confined electromagnetic field intensity is greatest, the resonant coupling of light into the crystal is modified, so the reflected/transmitted output is tuned. The highly confined electromagnetic field within a photonic crystal structure provides high sensitivity and a high degree of spatial resolution consistent with their use in imaging applications, much like fluorescent imaging scanners.

Photonic crystal structures have their historical roots in a phenomenon called "Wood's anomaly." Wood's anomalies are effects observed in the spectrum of light reflected by optical diffraction gratings.[15] They manifest themselves as rapid variations in the intensity of particular diffracted orders in certain narrow frequency bands. They were first discovered by Wood in 1902 during some of the first experiments on reflection gratings and were termed *anomalies* because the effects could not be explained by ordinary grating theory. Since that time, optical theory and numerical methods have

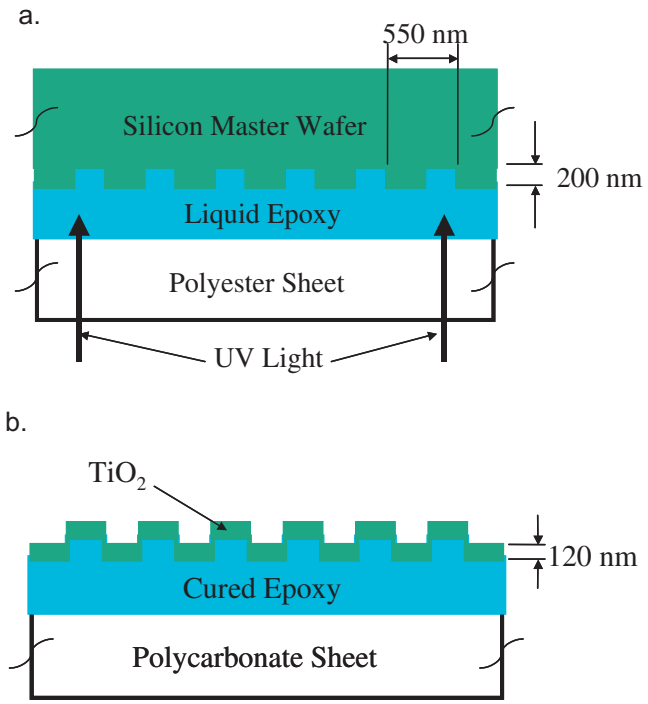

FIG. 1. Fabrication process used to produce the sensor on continuous sheets of plastic film. First (**a**), the silicon master wafer is used to replicate the sensor structure into a thin film of epoxy between the silicon and a sheet of plastic film. After the epoxy is cured, the plastic sheet is peeled away. To complete sensor fabrication (**b**), a thin film of titanium oxide is deposited over the structure.

developed so that structures making use of this optical effect could be engineered to produce useful devices in the fields of telecommunications and optical displays.[16] For example, GMRFs have been developed using Wood's effect to produce devices that, when illuminated with white light, are designed to reflect only a very narrow band of wavelengths.[13] To create a biosensor, a guided-mode resonant filter design may be optimized to provide an extremely narrow resonant mode whose wavelength is particularly sensitive to modulations induced by the deposition of biochemical material on its surface.[5] A sensor structure, shown in Figure 1b, consists of a low-refractive index plastic material with a periodic surface structure that is overcoated with a thin layer of high-refractive dielectric material. Device structures based on linear gratings and 2-dimensional gratings (i.e., arrays of holes, posts, or veins arranged in checkerboard or hexagonal close-packed grids along the sensor surface) have been demonstrated. The sensor is measured by illuminating the surface with white light and collecting the reflected light with a noncontact optical fiber probe, where several parallel probes can be used to independently measure different locations on the sensor. The biosensor design enables a simple manufacturing process to produce sensor sheets in continuous rolls of plastic film that are hundreds of meters in length.[17] The mass manufacturing of a biosensor structure that is measurable in a noncontact mode over large areas enables the sensor to be incorporated into single-use disposable consumable items such as 96-, 384-, and 1536-well standard microplates, thereby making the sensor compatible with standard fluid-handling infrastructure employed in most laboratories.

The sensor operates by measuring changes in the wavelength of reflected light as biochemical binding events take place on the surface. For example, when a protein is immobilized on the sensor surface, an increase in the reflected wavelength is measured when a complementary binding protein is exposed to the sensor. Using low-cost components, the readout instrument is able to resolve protein mass changes on the surface with resolution less than 1 pg/mm^2. Although this level of resolution is sufficient for measuring small molecule interactions with immobilized proteins, the dynamic range of the sensor is large enough to also measure larger biochemical entities, including live cells, cell membranes, viruses, and bacteria. A sensor measurement requires ~20 msec, so large numbers of interactions can be measured in parallel, and kinetic information can be gathered. The reflected wavelength of the sensor can be measured in "single-point mode" (such as for measuring a single interaction within a microplate), or an imaging system can be used to generate an image of a sensor surface with ~13-micron resolution. The "imaging mode" can be used for applications that increase the overall resolution and throughput of the system, such as label-free microarrays, imaging plate reading, self-referencing microplates, and multiplexed spots/well.[18]

Sensor fabrication

The sensor structure uses a grating with a period lower than the wavelength of the resonantly reflected light. Structures reported here contain a linear grating with a period of 500 nm and a depth of ~170 nm. The grating was microreplicated from a silicon wafer etched with a negative of the sensor surface structure acting as a mold for a layer of ultraviolet light-cured resin that is squeezed between the silicon and a polyester sheet,[17] as shown in Figure 1. After the resin is cured, the solid surface structure is peeled away from the silicon wafer, leaving behind a perfect replica of the silicon wafer surface adhered to the polyester sheet. Sensor fabrication is completed by sputter deposition of a high-refractive index dielectric coating of titanium oxide to yield the completed structure. Both the replication and dielectric coating processes are performed on continuous sheets of plastic film that are hundreds of meters in length. Completed sensors are cut from the plastic sheet and attached with adhesive to bottomless 96- or 384-well microplates, as shown in Figure 2.

Readout instrument

A schematic diagram of the system used to illuminate the sensor and to detect the reflected signal is shown in Figure 3. To excite the reflected resonance, a white light source illuminates a ~2-mm diameter region of the grating surface through a 400-µm diameter fiber optic and a collimating lens at nominally normal incidence

FIG. 2. Photo of a Biomolecular Interaction Detection (BIND) sensor embedded into the bottom surface of a standard 96-well microplate; 384-well BIND microplates have also been developed.

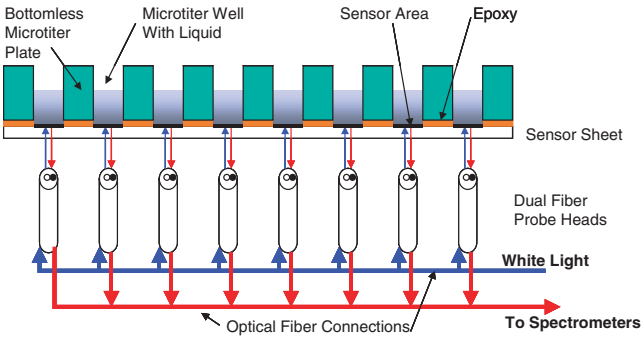

FIG. 3. Instrumentation used to illuminate and to read the output of the sensor structure. Eight separate probe heads are arranged to read an entire column of a microplate at once. Each probe head contains 2 optical fibers. The first fiber is connected to a white light source to cast a small spot of collimated light onto the sensor surface, and the second fiber collects reflected light for analysis by a spectrometer.

through the bottom of the microplate. A detection fiber for gathering reflected light is bundled with the illumination fiber for analysis with a spectrometer. A series of 8 illumination/detection heads are arranged in a linear fashion, so that reflection spectra are gathered from all 8 wells in a microplate column at once. The microplate sits on a motion stage so that each column can be addressed in sequence. The instrument is capable of measuring all 96 wells in ~15 sec. More rapid kinetic information can be gathered from a subset of the plate, where a single column can be measured at 0.5-sec intervals.

Using the above sensor structure and illumination/detection approach, the narrowband resonant reflectivity characteristic shown in Figure 4 is obtained from every location on the sensor surface. The sensor acts as a perfectly reflecting mirror at the resonant wavelength while all other wavelengths are allowed to transmit

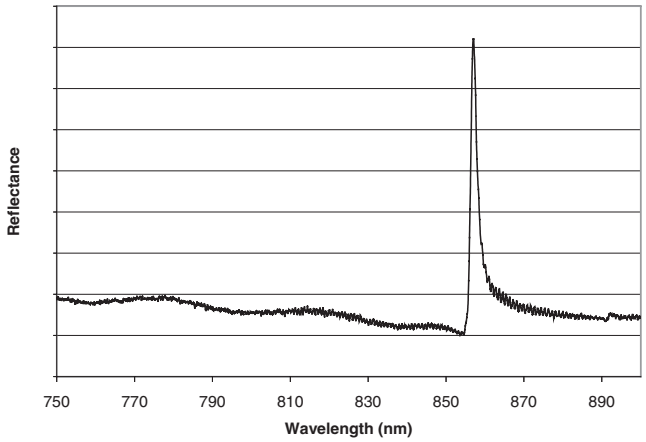

FIG. 4. Reflected intensity as a function of wavelength for the sensor structure within a microplate well filled with water.

through. Because the resonant reflection occurs only for a very narrow band of wavelengths, the peak wavelength value (PWV) can be measured with high precision. The adsorption of any biochemical material (small molecules, DNA, protein, viruses, cells) on the sensor results in a net increase of the dielectric permittivity of the surface, which in turn causes the PWV to shift to greater wavelengths. We have demonstrated that the magnitude of PWV shift produced by the adsorption of material is linear up to ~ΔPWV = 20 nm.[19] Compared with the minimum measured noise in ΔPWV, which can be as low as 0.0005 nm in standard deviation, we arrive at a dynamic range of up to 40,000. With this dynamic range magnitude, the system is capable of reporting signals that are directly proportional to the adsorbed mass for small molecules, proteins, and cells. For all the assays demonstrated in this work, we report the *shift* in PWV in units of reflected *wavelength* (nanometers, nm) as the detected quantity.

RESULTS

Because the BIND sensor is capable of detecting the adsorption/desorption of any biochemical material on its surface, it can be used as a general-purpose platform for performing a wide variety of assays. In this section, a small number of exemplary applications are described in which the BIND system is used to characterize a protein-protein interaction, to characterize protein–small molecule interactions, to measure toxicity of drugs on cells, and to characterize protein expression by cells. For each example, 96-well BIND microplates and the 8-channel optical fiber probe (single measurement point per well) instrument were used.

Protein-protein interaction

As a simple illustration of the operation of the BIND system and the uniformity of the sensor, the interaction of protein A with

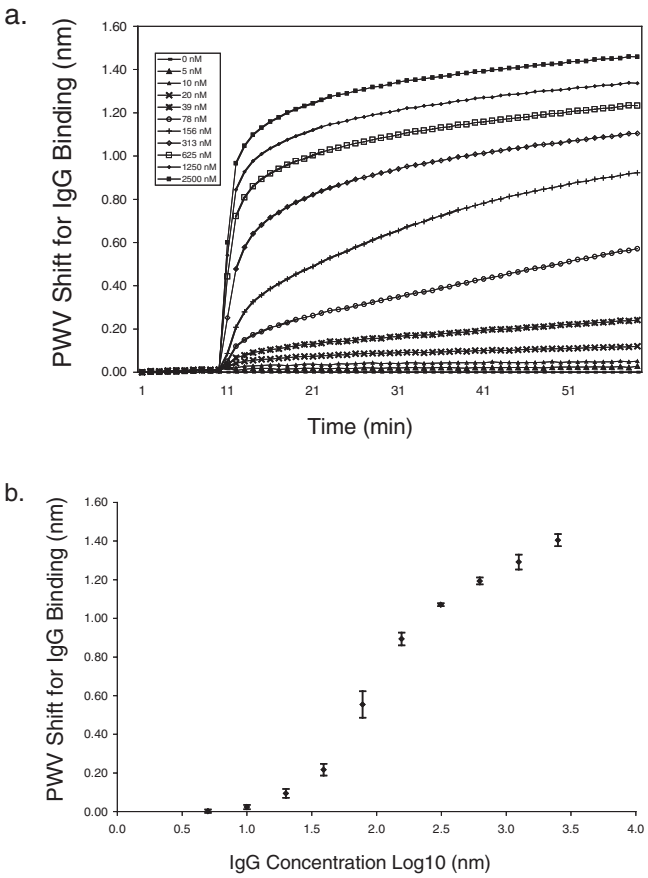

FIG. 5. (**a**) Kinetic response of a Biomolecular Interaction Detection (BIND) microplate with a protein A–coated surface to a range of IgG concentrations and (**b**) endpoint plot of the same data taken after a 60-min IgG exposure, with error bars shown for each condition measured with $n = 7$ replicate wells.

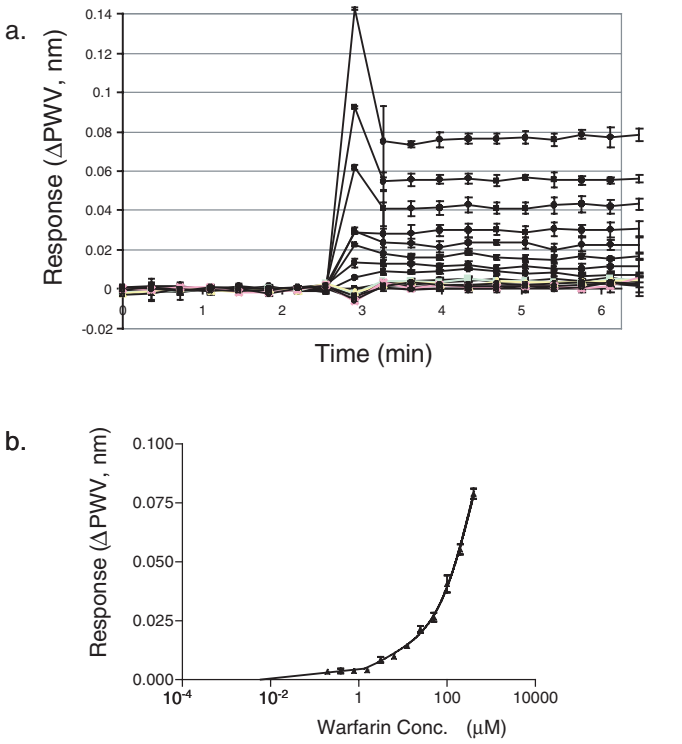

FIG. 6. Application of the Biomolecular Interaction Detection (BIND) system for the human serum albumin (HSA)warfarin model system. (**a**) Kinetic response measured for a range of exposed warfarin concentrations, simultaneously exposed to the HSA-immobilized sensor surface at t = 3 min. (**b**) Response data at equilibrium obtained (t = 5 min) after the addition of warfarin (*x*-axis on a log scale).

human IgG was characterized. A partial monolayer of protein A was applied to 10 columns of a 96-well BIND microplate by adding 100 µL of a 100-µg/mL solution of protein A in phosphate-buffered saline (PBS) to each well and allowing the solution to incubate on the surface for 30 min. Column 1 of the microplate was reserved as a baseline reference, although a single well may be used as a negative control for the whole plate. Following the removal of the protein A solution and washing the wells with PBS, a positive PWV shift of 0.341 nm was observed. Next, human IgG solutions with concentrations ranging from 1 to 2500 nM were added to the wells. Each concentration condition was replicated in 7 wells. The kinetic PWV response of the protein A–coated sensors for IgG exposure is shown in Figure 5a. Using the endpoints of this measurement at the 50-min time point, Figure 5b is generated with error bars representing the standard deviation of 7 replicates. The BIND system, therefore, enables very rapid and accurate characterization of a protein-protein binding interaction in a format that enables many interactions to be characterized rapidly in a high-throughput manner.

Small molecule–protein interaction

To demonstrate the capabilities of the BIND sensor in measuring small molecule interactions, human serum albumin (HSA, 66 kDa) binding warfarin (308 Da) and carbonic anhydrase II (CA II, 30 kDa) binding 4-carboxybenzene sulfonamide (CBS, 201 Da) were used as model systems. The model systems were selected to demonstrate the potential utility of the BIND system for small molecule drug screening. Both of these systems are well characterized and have been extensively studied using optical biosensors.[20-22]

For the HSA-warfarin model system, HSA was immobilized on a BIND 96-well sensor plate.[23] The estimated shift in peak wavelength value for HSA immobilization was 8 nm. Samples containing warfarin (0.12-400 µM) in PBS with 1% DMSO (PBS-D) were diluted 10-fold into wells containing PBS-D. Each concentration was assayed in quadruplicate, and the binding response was recorded at equilibrium. Figure 6a shows the average change in PWV over time as different concentrations of warfarin are added to

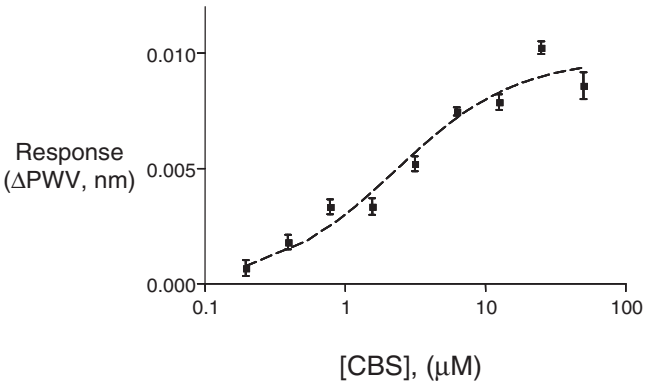

FIG. 7. Application of the Biomolecular Interaction Detection (BIND) system for the CA II–CBS model system. Endpoint response dose-response characterization measured for a range of CBS (mol. wt. = 201 Da) concentrations. CA II, carbonic anhydrase II; CBS, 4-carboxybenzene sulfonamide.

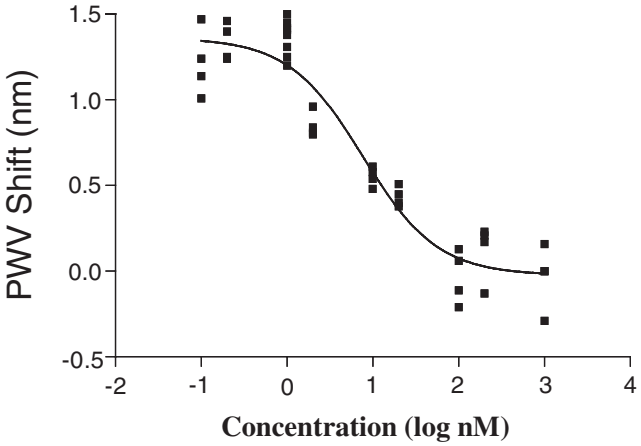

FIG. 8. Dose-response characterization of Chinese hamster ovary (CHO) cell proliferation on the Biomolecular Interaction Detection (BIND) sensor surface, as modulated by the introduction of a range of concentrations of vinblastine. Points were fit to this line using Graphpad Prism nonlinear regression sigmoidal dose response.

the wells. Figure 6b shows the equilibrium binding response plotted versus the concentration of warfarin and fit to a 2-site binding model. HSA has multiple binding sites for warfarin. The equilibrium data were fit to a 2-independent-binding-sites model, yielding apparent equilibrium dissociation constants of 2.9 ± 1.5 and 398 ± 113 μM for the high- and low-affinity sites, respectively. These values correlate well with the values of 3.8 μM and 273 μM reported in the literature.[22]

For the CA II–CBS model system, the CA II protein was covalently immobilized onto an aldehyde functionalized BIND 96-well sensor plate via hydrazide coupling chemistry. CA II was immobilized in a volume of 50 μL at a concentration of 50 μg/mL. The mean peak wavelength shift (ΔPWV) for the immobilization was 2.39 nm, with coefficient of variation (CV) = 5.8%. Wells lacking CA II were reserved as reference surfaces for the subsequent binding assays to correct for bulk refractive index changes and any nonspecific binding of the analyte to the aldehyde surface. Samples containing CBS (2-500 μM) were diluted 10-fold into wells containing PBS. Nonspecific binding was not observed. Each concentration was assayed in quadruplicate, and the binding response was recorded after the signal had plateaued. Figure 7 shows the endpoint response plotted versus concentration of CBS (*x*-axis plotted on a log scale) and fit to a simple 1:1 binding model yielding an apparent equilibrium dissociation constant of 2.3 0.5 μM. The literature value reported for this interaction is 0.76 μM.[21]

Cytotoxicity

In addition to accurately detecting the adsorption of proteins and subsequent small molecule interactions on the sensor surface, the BIND system also demonstrates the ability to precisely track cell density. Adherent cell lines, such as Chinese hamster ovary cells (CHO-K1), readily attach to the unmodified sensor surface, where the density of attached cells can be measured quantitatively within a linear detection range extending from 775 to 40 cells/mm^2. The BIND system can also rapidly and quantitatively measure cell attachment, proliferation, and cell death without the use of fluorescent markers, which may require cell fixation before measurement by optical microscopy.

In previous work, the antiproliferation agent, vinblastine sulfate, modulated cell adherence.[24] This drug causes metaphase arrest of mitosis, resulting in cell detachment from surfaces and cell death.[25] Using the BIND system, the CHO-K1 cell proliferation on the sensor surface can be measured by introducing 5.0×10^3 cells/well in complete F12-K media and monitoring the increase in PWV after a time period of 36 h. Upon addition of 0.1 nM to 200 μM vinblastine to those BIND wells with CHO-K1 cells bound to the sensor surface, the IC_{50} of vinblastine can be calculated as shown in Figure 8. The BIND system IC_{50} determination of 8.31 nM vinblastine for CHO-K1 cells is comparable to those values obtained using the MTT Assay and Oxygen BioSensor with HL60 cells, where the reported IC_{50} = 11 nM.[26]

Protein-cell interaction

Identification of protein-cell interactions will help to elucidate the mechanisms that are involved in cellular functions, such as inflammation, wound healing, cancer metastasis, cell differentiation, and migration. Current techniques for studying protein-cell interactions can be time-consuming and labor intensive. Common practice usually involves many steps, including radioisotope or fluorescence labeling, blocking, washing, and detecting. We have developed a label-free biosensor-based cell attachment assay that can be used to monitor cell interaction with specific antibodies or natural ligands coated on a BIND sensor.

The BIND cell attachment assay includes 2 steps: coating the sensor surface with antibody and detecting cell attachment through

affinity binding of cell surface molecules to the immobilized antibody (or natural ligands). Monoclonal antibodies in this study were purchased from R & D Systems, Inc. and included anti–human CD3 (MAB100), anti–human CD28 (MAB342), anti–human CD45 (MAB1430), anti–human CTLA4 (cytotoxic T lymphocyte–associated molecule-4, MAB325), control isotype antibodies, and anti–mouse CD3 antibodies (MAB484). Antibodies were immobilized on the BIND sensor surface by using 1 μg/well of different monoclonal antibodies. After removing and rinsing the sensor surface with immobilization buffer, the coated sensor surface was incubated with cell culture media RPMI1640, supplemented with 10% fetal bovine serum (ATCC 30-2020) and penicillin-streptomycin glutamine (Sigma, P0781). Two T lymphocyte cell lines, Jurkat E6-1 (ATCC, TIB-152) and J45.01 (ATCC, CRL-1990), were maintained in RPMI1640 culture media as suggested by ATCC. Cells were harvested and resuspended at 5×10^6 cells/mL in fresh RPMI complete media. Then, 5×10^5 cells were added into antibody-coated wells. The interaction of specific antibody and cell surface antigen was monitored in real time as lymphocytes were binding to the coated sensor surface. The binding of cells to the antibody-coated sensor was clearly detected only when the corresponding antigen was expressed on the Jurkat cell surface. As shown in Figure 9, both JE6-1 and J45.1 interact well with anti-CD3- and anti-CD28-coated BIND sensor surfaces. However, both cell lines show lower level binding to anti-CTLA-4 antibody. Those results were confirmed by flow cytometry experiments, in which JE6-1 and J45.1 show high-level expression of CD3 and CD28 but much lower expression of CTLA-4. BIND signals were significantly different for JE6-1 and J45.01 interaction with the anti-CD45 antibody. The binding signal for J45.01 was only 9% in comparison to the signal of Jurkat E6-1 with the anti-CD45 antibody. Interestingly, CD45 expression level on the J45.01 cell surface has been previously reported at only 8% of the cells expressing CD45 in comparison with the wild-type E6-1 cells. These experimental results demonstrate that the BIND cell attachment assay can be used to characterize proteincell surface interactions.

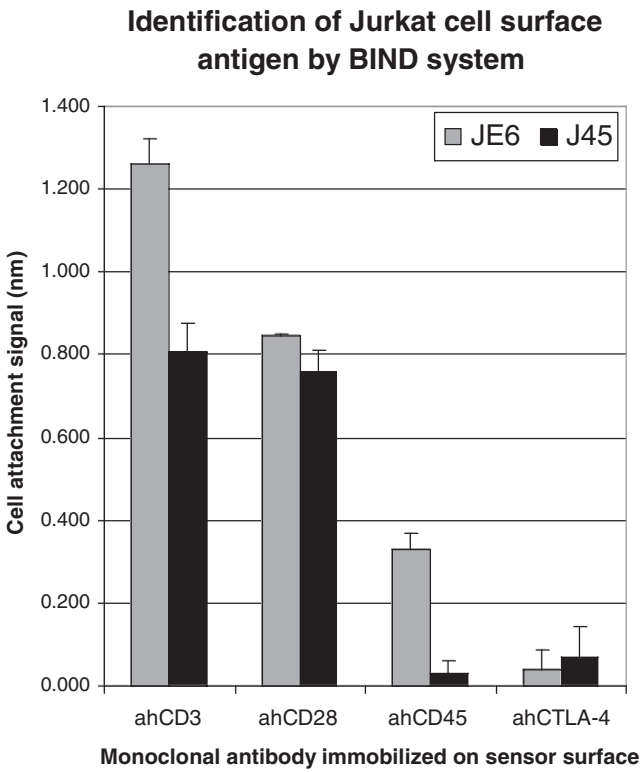

FIG. 9. Identification of cell surface antigen by the Biomolecular Interaction Detection (BIND) cell attachment assay. Jurkat cells (5×10^5) were added in the wells that have been coated with anti–human CD3, anti–human CD28, anti–human CD45, and anti–human CTLA-4 monoclonal antibodies. Cell attachment was detected using the BIND microplate reader in real time. After a 60-min incubation, unattached cells were removed and the plate was washed with RPMI1640 complete growth media. Endpoint cell attachment was analyzed using BIND EMS software. Solid bars represent Jurkat E6-1 cell, and striped bars represent cell attachment data collected from J45.01.

DISCUSSION

As shown in the previous section, the BIND system is a versatile tool that can be applied to several different types of assays. The current microplate-based format allows compatibility with the liquid-handling infrastructure for plate filling, aspirating, washing, incubating, storage, stacking, and robotic transfer between instruments. Although the microplate format does not allow for liquid flow, multiple wells within a plate can be used to rapidly obtain dose-response characteristics, which in turn can be used to accurately determine affinity-binding coefficients using diffusion-based equilibrium binding kinetics. Because the microplate is scanned in <15 sec, kinetic binding characteristics can be easily observed. Alternatively, the BIND plate can be located off-stage during the binding phase for determination of PWV shifts by endpoints only.

Managing sources of error

As with other optical biosensors, the effects of temperature, bulk refractive index of the sample, drift, and nonspecific binding can result in a measurable signal that is not due to the binding interaction of interest. Using the fiber probe–based instrument described in Figure 3, the entire well yields 1 measurement from a ~2-mm diameter circle in the center of the well. Therefore, reference wells are typically designated to provide a negative control measurement for the "live" assay wells. For this type of reference method, the minimum observable PWV shift that can be classified as a signal due to binding can be determined by the uniformity of the error from 1 well to another within the plate. Due to the high level of uniformity afforded by the roll-based sensor manufactur-

ing process and by the sensor surface treatment, non-uniformity-based errors can be controlled to a level that is compatible with the Z' targets required for a screening campaign. Results characterizing the Z' of binding assays as a function of the detected molecular weight will be described in an upcoming publication. The well-to-well referencing method can be further improved on by incorporating active and reference regions within each well. The imaging readout instrument, described below, represents a next-generation detection method that provides "self-referencing" capabilities for automatically compensating for bulk, thermal, and nonspecific binding effects without the need for separate reference wells.

Imaging readout instrument

The single-point illumination/single-point spectrometer detection method described above can be extended to incorporate an imaging spectrometer that is capable of generating high-resolution spatial maps of the PWV on the biosensor surface. Using this instrument, it is possible to observe patterns of biomolecule receptor attachment and hybridization interactions with high density. Because white light illumination is used, and because there is no optical contact required (such as a coupling prism) to the sensor, the imaging method can be performed on large sensor areas such as entire microplates and microarray slides. As the same biosensor structure and peak-detecting method are used for single-point-based and imaging-based detection, the sensitivity (in terms of amount of PWV shift observed and resolution of PWV shift detection) of the approach is not compromised.

A schematic diagram of the biosensor PWV imaging instrument is shown in Figure 10. White light illuminates the sensor at normal incidence with a polarization filter to apply only light with polarization direction perpendicular to the sensor grating lines. The reflected light is directed through a beam splitter and an imaging lens to a narrow slit aperture at the input of an imaging spectrometer. Using this method, reflected light is collected from a line on the sensor surface, where the width of the imaged line is determined by the width of the entrance slit of the imaging spectrometer. The imaging spectrometer contains a 2-dimensional CCD camera with 2048×512 pixels. The line of reflected light, containing the biosensor resonance signal, is diffracted by a diffraction grating to produce a spatially resolved spectrum from each point within the line. When the CCD camera is operated in 2048×512 pixel mode, the line image through the slit is imaged onto 512 pixels. A spectrum, with a resolution of 2048 wavelength data points, is acquired for each of the 512 pixels. Upon peak-finding analysis of all 512 spectra, the PWVs of 512 pixels are determined. Thus, a line of 512 pixels is generated for the PWV image of the sensor.

To generate a 2-dimensional image of the sensor, a motorized stage translates the sensor in the direction that is perpendicular to the image line. The spatial separation of the image lines is determined by the step size of the stage between each image line acquisition. By this technique, a series of lines is assembled into an image through software. In the current system, the length of the

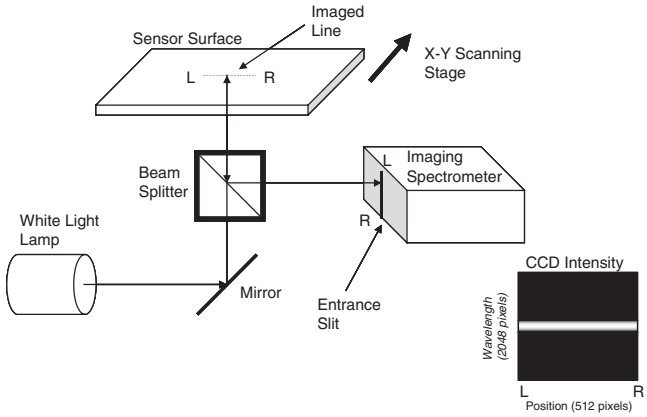

FIG. 10. Schematic diagram of the imaging Biomolecular Interaction Detection (BIND) readout instrument. The optical fiber-based illumination/detection system is replaced with an imaging spectrometer capable of rapidly scanning the peak wavelength value (PWV) of large sensor surface areas, with spatial resolution demonstrated down to 13 mm.

image line is ~3 inches, as determined by the width of a microplate. A large area can be scanned by translating the sensor in steps along the image line direction. The scanning can be performed rapidly so that an entire microplate can be imaged in 30 sec for 150×150-μm pixel resolution. The scan rate is determined predominantly by the time required to read the PWV spectra from the CCD chip. Therefore, reduction of pixel size for higher resolution images results in proportionally longer scan time for a given surface area. The highest resolution images demonstrated to date by this method were gathered with 13×13-μm pixels, as limited by the pixel size of the CCD chip.[18] Fundamentally, the spatial resolution is limited to the lateral optical confinement of the photonic crystal, which can be as low as 3 to 5 μm with the structures reported here.

Typically, a biosensor experiment involves measuring shifts in PWV, so the sensor surface is scanned twice, once before and once after biomolecular binding. The images are aligned and subtracted to determine the shift in PWV as detected by the sensor. This scanning method does not require the PWV of the imaged surface to be completely uniform, either across the surface or within a set of probe locations, or the sensor angle to be tuned to a resonance condition as with SPR imaging. As an example, Figure 11a shows a PWV shift image of a BIND 384-well plate taken with the imaging readout instrument, where protein was adsorbed onto selected wells to induce a ~1-nm positive shift. In Figure 11b, a single 7-mm diameter microplate well is imaged with 50-μm resolution to measure the PWV shift of 62 separate spots within the well. In this case, alternating rows of high-density and low-density spots were produced with a ~400-μm diameter, where the high-density spots produced a PWV shift of ~1 nm.

The imaging capability allows hundreds of independent PWV measurements within a well of a BIND microplate. In addition to the ability to multiplex many assays within a well, the number of

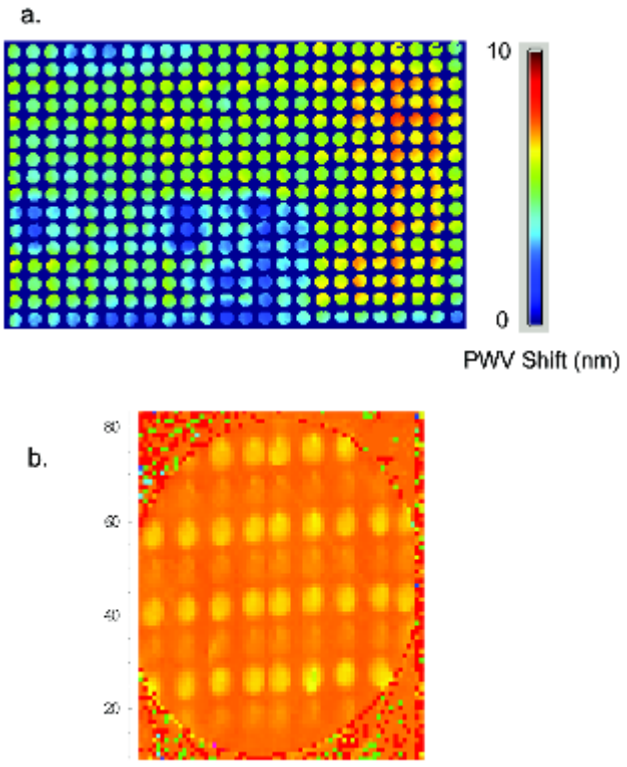

FIG. 11. Example PWV shift images gathered with the Biomolecular Interaction Detection (BIND) imaging instrument, where brighter regions represent areas of greater peak wavelength value (PWV) shift. (**a**) A BIND 384-well plate, scanned at 300-mm pixel resolution in ~30 sec, where the PWV was shifted by the adsorption of a protein to selected wells. (**b**) BIND image of a single 7-mm diameter microplate well with 62 separate spots of alternating rows of adsorbed IgG and collogenase.

independent measurements can also be used to increase Z' scores of assays performed using the entire well surface and to provide internal reference locations for bulk refractive index errors. The imaging readout approach also extends the BIND microplate reader capability to 1536-well plates, microarrays, and multiparallel flow channel devices. We plan to present assay results using the BIND imaging readout instrument in a future publication.

CONCLUSIONS

With the BIND system, we have developed a highly sensitive label-free assay system using an optical biosensor based on a guided-mode resonant filter phenomenon. The sensor is inexpensively manufactured in large volumes from continuous sheets of plastic film and incorporated into standard-format 96- and 384-well microplates for compatibility with automated liquid-handling equipment and other laboratory infrastructure. The readout instrument is simple, robust, and capable of interfacing with automated microplate-handling systems. The system offers a sensor format that is compatible with the needs of pharmaceutical screening laboratories from a sensitivity, cost/assay, and throughput standpoint for several types of assay applications, including protein interaction characterization, small molecule screening, and cell-based assays. Advanced versions of the sensor microplates and instrumentation are under development that take advantage of the high-resolution imaging capabilities of the sensor to enable higher limits of throughput and accuracy to be obtained.

REFERENCES

1. Brecht A, Gauglitz G: Optical Probes and transducers. *Biosens Bioelectron* 199;10:923-936.
2. Cunningham AJ: *Introduction to Bioanaytical Sensors*. New York: John Wiley, 1998.
3. Arakawa T, Kita Y: Refractive index of proteins in organic solvents. *Anal Biochem* 1999;271:119-120.
4. Nelson BP, Frutos AG, Brockman JM, Corn RM: Near-infrared surface plasmon resonance imaging measurements of ultrathin films: 1. Angle shift and SPR imaging experiments. *Anal Chem* 1999;71:3928-3934.
5. Cunningham BT, Li P, Lin B, Pepper J: Colorimetric resonant reflection as a direct biochemical assay technique. *Sens Actuators B* 2002;81:316-328.
6. Haes AJ, Duyne RPV: A nanoscale optical biosensor: sensitivity and selectivity of an approach based on the localized surface plasmon resonance spectroscopy of triangular silver nanoparticles. *J Am Chem Soc* 2002;124:10596-10604.
7. Joannopoulos JD, Meade RD, Winn JN: *Photonic Crystals*. Princeton, NJ: Princeton University Press, 1995.
8. Munk BA: *Frequency Selective Surfaces*. New York: John Wiley, 2000.
9. Pacradouni V, Mandeville WJ, Cowan AR, Paddon P, Young JF, Johnson SR: Photonic band structure of dielectric membranes periodically textured in two dimensions. *Phys Rev B* 2000;62(7):4204-4207.
10. John S: Strong localization of photons in certain disordered dielectric superlattices. *Phys Rev Lett* 1987;58(23):2486-2489.
11. John S, Rupasov VI: Multiphoton localization and propagating quantum gap solitons in a frequency gap medium. *Phys Rev Lett* 1997;79(5):821-824.
12. Scherer A, Yoshie T, Loncar M, Vuckovic J, Okamoto K, Deppe D: Photonic crystal nanocavities for efficient light confinement and emission. *J Korean Phys Soc* 2003;42:768-773.
13. Magnusson R, Wang SS: New principle for optical filters. *Appl Phys Lett* 1992;61(9):1022-1024.
14. Magnusson R, Wang SS: Transmission bandpass guided-mode resonance filters. *Appl Optics* 1995;34(35):8106-8109.
15. Wood RW: On a remarkable case of uneven distribution of light in a diffraction grating spectrum. *Philos Mag* 1902;4:396-402.
16. Hessel A, Oliner AA: A new theory of Woods anomalies on optical gratings. *Appl Optics* 1965;4(10):1275-1297.
17. Cunningham BT, Qiu J, Li P, Pepper J, Hugh B: A plastic colorimetric resonant optical biosensor for multiparallel detection of label-free biochemical interactions. *Sens Actuators B* 2002;85:219-226.
18. Li P, Lin B, Gerstenmaier J, Cunningham BT: A new method for label-free imaging of biomolecular interactions. *Sens Actuators B* 2003;1:310-315.
19. Cunningham BT, Qiu J, Li P, Baird C: Enhancing the surface sensitivity of colorimetric resonant optical biosensors. *Sens Actuators B* 2002;87(2):365-370.

20. Frostell-Karlsson A, Remaeus A, Roos H, Andersson K, Borg P, Hamalainen M, et al: Biosensor analysis of the interaction between immobilized human serum albumin and drug compounds for prediction of human serum albumin binding levels. *J Med Chem* 2000;43(10):1986-1992.
21. Day YS, Baird CL, Rich RL, Myszka DG: Direct comparison of binding equilibrium, thermodynamic, and rate constants determined by surface- and solution-based biophysical methods. *Protein Sci* 2002;11(5):1017-1025.
22. Rich RL, Day YS, Morton TA, Myszka DG: High-resolution and high-throughput protocols for measuring drug/human serum albumin interactions using BIACORE. *Anal Biochem* 2001;296(2):197-207.
23. Hermanson GT: *Bioconjugate Techniques*. San Diego: Academic Press, 1996.
24. Lukenbill-Edds L, Kleinman HK: Effect of laminin and cytoskeletal agents on neurite formation by NG108-15 cells. *J Neurosci Res* 1988;19(2):219-229.
25. Wendell KL, Wilson L, Jordan MA: Miotic block in HeLa cells by vinblastine: ultrastructural changes in kinetochore-microtubule attachment and in centrosomes. *J Cell Sci* 1993;104:261-274.
26. Wodnicka M, Guarino RD, Hemperly JJ, Timmins MR, Stitt D, Pitner JB: Novel fluorescent technology platform for high throughput cytotoxicity and proliferation assays. *J Biomol Screen* 2000;l5(3):141-152.

Address reprint requests to;
Brian T. Cunningham
SRU Biosystems
14A Gill Street
Woburn, MA 01801

E-mail: bcunningham@srubiosystems.com